LWT - Food Science and Technology 217 (2025) 117316

Contents lists available at ScienceDirect

LWT

journal homepage: www.elsevier.com/locate/lwt

Free radical scavenging kinetics of Maillard reaction products: A glucose-glycine model system

Sara Bolchini [a], Lucrezia Angeli [a], Giovanna Ferrentino [a], M.A.J.S. Van Boekel [b], Riccardo Amorati [c], Matteo Scampicchio [a,*], Ksenia Morozova [a]

[a] Faculty of Agricultural, Environmental and Food Science, Free University of Bozen-Bolzano, Piazza Università 1, 39100, Bolzano, Italy
[b] Food Quality & Design, Wageningen University & Research, P.O. Box 17, 6700 AA, Wageningen, Netherlands
[c] Department of Chemistry "G. Ciamician", University of Bologna, Via S. Giacomo 11, I-40126, Bologna, Italy

ARTICLE INFO

Keywords:
Kinetic modeling
Electron transfer
Amadori compounds
Natural food additives
Redox reactions

ABSTRACT

This study investigated the free radical scavenging kinetics of Maillard reaction products (MRPs) generated from a glucose-glycine model system under controlled conditions (90 °C, pH 6.8) using a stopped-flow DPPH assay. Kinetic analysis revealed a time-dependent increase in antioxidant activity, highlighting the dynamic formation of reactive antioxidants during the Maillard reaction. Advanced analytical techniques, including high-performance liquid chromatography coupled with coulometric array detection (HPLC-CAD) and high-resolution mass spectrometry (HPLC-HRMS), were used to tentatively identify two key antioxidant MRPs: methylpyridin-3-ol (MP), 3,5-dihydroxy-6-methyl-2,3-dihydro-4H-pyran-4-one (DDMP) and its furanone isomer. The electrochemical properties of these compounds were evaluated, revealing their electron-donating abilities. A kinetic model was developed to simulate and predict the formation of these antioxidants, providing insights into the relationship between antioxidant reactivity and reaction progress. These findings contribute to our understanding of the formation of antioxidants during the Maillard reaction and offer a foundation for the development of natural antioxidants, which is aligned with the growing demand for clean-label food products.

1. Introduction

The Maillard Reaction (MR) plays a fundamental role in enhancing sensory attributes and preserving food quality. Maillard Reaction Products (MRPs) contribute to desirable characteristics, such as the toasted aroma of baked bread (Tang et al., 2024) and the golden-brown hue of grilled meat (Sun et al., 2023). In addition to these sensory qualities, MRPs exhibit significant antioxidant properties due to the formation of compounds, such as Amadori products and α-dicarbonyl compounds, which either possess reductone structures or can tautomerize into reductones, functioning similarly to ascorbic acid (Feng et al., 2022; Nooshkam et al., 2019; Shakoor et al., 2022). This antioxidant properties are connected to the development of flavours and aromas during the MR, in particular with umami flavour (Habinshuti et al., 2019; M. Yu et al., 2018). The antioxidant activityhelps inhibit lipid oxidation and prevents the degradation of essential nutrients through various mechanisms, including radical scavenging and metal chelation (Feng et al., 2022; Kanzler et al., 2016). This dual functionality, both sensory and antioxidant, makes MRPs valuable in preserving food quality during processing and storage (Han et al., 2022; Nooshkam et al., 2019; Sun et al., 2022). Moreover, recent interest in MRPs has grown due to their potential role in developing 'clean label' food products, which prioritize the use of natural compounds over synthetic additives for preservation (Jia et al., 2023; Kitts, 2021; Mildner-Szkudlarz et al., 2023; Monti et al., 1999). Understanding MRPs role in both sensory enhancement and antioxidant activity is therefore a key-strategy to develop natural food preservation techniques.

Despite significant progress in characterizing the sensory benefits of MRPs, the mechanisms underlying their antioxidant reactivity remain poorly understood (Cao et al., 2022; Feng et al., 2022; Sohail et al., 2022). Antioxidants prevent oxidative reactions that degrade essential nutrients, such as unsaturated fatty acids, vitamins, and pigments. However, a common misconception is that antioxidant activity is often assessed by concentration, whereas it is more accurately determined by the rate of radical scavenging reactivity (Angeli et al., 2021). This misconception likely arises from the widespread use of assays that

* Corresponding author.
E-mail address: matteo.scampicchio@unibz.it (M. Scampicchio).

https://doi.org/10.1016/j.lwt.2024.117316
Received 17 September 2024; Received in revised form 29 December 2024; Accepted 31 December 2024
Available online 1 January 2025

express antioxidant activity in terms of equivalent concentration, such as the thiobarbituric acid (TBA) assay, thiobarbituric acid reactive substances (TBARS) assay, and the β-carotene bleaching assay, which focus on the inhibition of lipid oxidation. Additionally, scavenging capacity is also expressed in terms of equivalent concentration through assays, such as 2,2-diphenyl-1-picrylhydrazyl (DPPH) (Foti, 2015), and oxygen radical absorption capacity (ORAC) (Asma et al., 2024). While these methods are useful, they may not fully capture the reactivity of antioxidants to neutralize radicals. Thus, antioxidant reactivity, rather than concentration alone, is crucial for determining their effectiveness (Amorati et al. 2018).

This study investigated the antioxidant reactivity of MRPs formed in a glucose-glycine model system to evaluate their formation and reactivity under controlled conditions (90 °C, pH 6.8). The objectives of this study are to (1) evaluate the antioxidant efficiency of MRPs using kinetic-based DPPH assays; (2) identify the most potent antioxidants through high-performance liquid chromatography (HPLC) coupled with coulometric array detection (CAD); (3) elucidate their electrochemical properties and tentatively identify their chemical structures using high-resolution mass spectrometry (HRMS); and (4) propose a kinetic model that predicts antioxidant formation under the experimental conditions.

This research could offer new insights into the mechanisms of antioxidant reactivity in MRPs, potentially contributing to the development of food products with improved nutritional and functional properties. Furthermore, it could offer a natural alternative to synthetic additives, in line with the growing demand for clean-label food products.

2. Experimental methods

2.1. Chemicals and reagents

All chemicals and reagents used in this study were of analytical grade. Sodium hydroxide, alpha-D-glucose (≥98%), fluorescein, Trolox, gallic acid, ascorbic acid, and potassium phosphate monobasic were obtained from Sigma-Aldrich (USA). Glycine (≥98.5%) was supplied by Alfa Aesar (USA) and potassium phosphate dibasic trihydrate were obtained from Amresco (USA). Mass spectrometry-grade methanol, acetic acid, deuterated water (D_2O), and trimethylsilylpropanoic acid were procured from Merck (Germany). Milli-Q water was produced using a Sartorius arium® mini system (Germany).

2.2. Maillard reaction model

The Maillard reaction (MR) was studied using a glucose-glycine model system. Equimolar solutions (200 mmol/L) of glucose and glycine were prepared in 0.1 mol/L phosphate-buffered saline (PBS) at pH 6.8, following the protocol described by (Martins & Van Boekel, 2005). The solution was divided into 9 Pyrex flasks with a maximum volume of 15 mL, sealed with hermetic stoppers, and stored overnight at 4 °C for equilibration. In each vial, 10 mL of the solution was poured, and the MR was initiated by immersing the 9 flasks in a water bath at 90 °C for 4 h, with a sample (1 vial) taken every 30 min. The samples were rapidly cooled in an ice bath to prevent further reaction and were stored at −80 °C to preserve their chemical integrity prior to analysis. All experiments were performed in triplicate.

2.3. Stopped flow DPPH assay (DPPH-kin)

The antioxidant kinetics were determined using a stopped-flow system (RX2000 Applied Photophysics, UK) coupled with a Cary 60 UV–Vis spectrophotometer (Agilent Technologies, USA). A solution of 200 μmol/L DPPH• in methanol/water (80:20) was mixed with an identical volume of an antioxidant standard (ascorbic acid or Trolox) or MRP samples, both at a concentration of 60 μmol/L gallic acid equivalents (GAE) quantified using Folin-Cicalteau method as described by Angeli (Angeli et al., 2024). The two solutions were rapidly mixed (mixing time less than 10 ms) and transferred into the flow cell, with a final concentration of 100 μmol/L DPPH• and 30 μmol/L GAE in the reaction mixture. Absorbance at 515 nm was measured every 18 ms. The molar extinction coefficient (ε_{515}) of DPPH• in methanol was 11,200 ± 400 mol^{-1} L cm^{-1}.

Since ascorbic acid and trolox react with Folin reagent in a ratio of approximately 0.5–0.6 and gallic acid equivalent ~ 1 (Everette et al., 2010), the 30 GAE μmol/L of MRPs corresponds to approximately 60 μmol/L of ascorbic acid. For this reason, MRPs were diluted to a concentration of ~30 GAE μmol/L prior to analysis, and reached a concentration of ~15–18 μmol/L in the reaction mixture.

The reaction kinetics were simulated using Copasi® software (version 4.34) with a three-step mechanism (eqs. (1)–(3)) (Friaa & Brault, 2006):

$$DPPH^{\cdot} + AH \underset{k_b}{\overset{k_{DPPH}}{\rightleftarrows}} DPPH\text{–}H + A^{\cdot} \quad (1)$$

$$DPPH^{\cdot} + A^{\cdot} \xrightarrow{k_{side}} \text{non radical product} \quad (2)$$

$$A^{\cdot} + A^{\cdot} \xrightarrow{k_{term}} \text{dimer} \quad (3)$$

The three steps mechanism was developed based on literature (Angeli et al., 2021; Foti & Daquino, 2006; Foti et al., 2004) and it is suitable to study the kinetics of reaction between DPPH• and complex samples like MR samples. However, it could be semplified for single and fast standard antioxidants like ascorbic acid or Trolox, where the main reaction (eq. (1)) is enough to describe the kinetics of the oxidation, since no side or equilibrium reactions occur.

Parameters k_{DPPH}, k_{side}, and k_{term} were optimized through iterative fitting using an evolutionary strategy (SRES) program. Fitting was performed using 200 generations and 24,000 function evaluations. All analyses were performed in triplicate, and the results were averaged for data presentation.

2.4. High performance liquid chromatography

HPLC analysis was performed using a 1260 Infinity HPLC system (Agilent Technologies, USA) equipped with a Kinetex Biphenyl column (100 × 2.1 mm, 2.6 μm particle size) and a pre-column. The mobile phases consisted of water with 0.5% acetic acid (v/v) (A) and methanol with 0.5% acetic acid (v/v) (B). The following gradient was used at a flow rate of 0.3 mL/min: 2% B from 0 to 5 min, 3% B from 5 to 9 min, 5% B from 9 to 16 min, and 2% B from 16 to 20 min. The injection volume was 10 μL, and samples were diluted 1:40 with phase A and filtered with polytetrafluoroethylene (PTFE) 0.2 nm filters prior to analysis.

Three detectors were used in parallel for sample analysis: a diode array detector (DAD), CoulArray detector (CAD), and high-resolution Q Exactive Orbitrap mass spectrometer (HRMS).

2.4.1. Diode array detector

DAD monitored absorbance from 210 to 600 nm, with a focus on the 280 nm absorption band, which corresponds to phenolic compounds and Maillard reaction products. The chromatograms were compared with the CAD and HRMS data.

2.4.2. Coulometric detector

Coulometry, an absolute electrochemical method, was employed using a 16-cell CoulArray detector (Thermo Fisher Scientific, USA). Each cell was set at increasing potentials, ranging from −200 mV to +650 mV in 50-mV increments to completely oxidize the analytes. Analyte concentrations were quantified based on the total charge transferred using Faraday's law (Razem et al., 2022). CAD chromatograms were collected and processed using CoulArray data station 3.10 and R software (version 4.1.2). The data were analyzed using the MALDIquant R package for

peak identification, peak height, and area calculations, as previously described (Ding et al., 2022).

2.4.3. High-resolution mass spectrometry

Tentative identification of antioxidants was performed using a Q-Exactive Orbitrap mass spectrometer (Thermo Fisher Scientific, USA). The electrospray ionization source (ESI) was operated in positive ionization mode with a capillary voltage of 4.00 kV, and a capillary temperature of 300 °C. The full MS scan was acquired from 50 to 750 m/z with a resolution of 70.000, an automatic gain control (AGC) target of 1×10^6 and maximum injection time of 100 ms. An inclusion list of targeted species was defined based on the full HRMS scan and used to run a data-dependent MS/MS analysis (MS/MS) to obtain the fragmentation patterns of each target specie. In this case, the AGC target was set at 5×10^5, the maximum injection time was 50 ms, and the resolution was 17,500 with an isolation window of 4.0 m/z. The collision energy used for the fragmentation was 15 eV. The spectrometer was calibrated every 48-h with Pierce LTQ Velos ESI-positive calibration solution (Thermo Fisher Scientific). The data were collected with Chromeleon 7.2 and analyzed with Xcalibur 4.3, Compound Discoverer 3.3 software, and Mass Frontier 7.0 software (Thermo scientific Scientific, MA, USA).

2.5. Hydrodynamic voltammogram

Hydrodynamic voltammetry was performed using CAD to measure the redox properties of the MRPs. The half-wave potential ($E_{1/2}$) and maximum charge (Q_{max}) were derived from the HDV, providing insights into the electron-donating capacity of MRPs. $E_{1/2}$ is indicative of antioxidant potential, with lower values correlating with stronger electron-donating capacity (Razem et al., 2022).

2.6. Nuclear magnetic spectroscopy

Acetic acid and formic acid were quantified using ^{1}H NMR, while glucose and glycine were measured using ^{13}C NMR due to signal overlap in ^{1}H NMR spectra. All spectra were acquired using a Jeol JNM-ECZ600R/M3 spectrometer at 25 °C. The quantification of each compound was performed by integrating the respective peaks and comparing them with an internal standard (TSP). Calibration curves for glucose and glycine were generated using concentrations ranging from 50 to 250 mmol/L, with an R^2 of 0.997 and 0.989, respectively.

2.7. Determination of melanoidins

Melanoidins were quantified at 470 nm using a microplate reader (Tecan Infinite M Nano+, Switzerland) following the method described by (Martins & Van Boekel, 2003). The extinction coefficient ($\varepsilon_{470} = 0.64$ mol^{-1} L cm^{-1}) and optical path length of 0.556 cm were used to calculate the molar melanoidin concentrations.

2.8. Kinetic analysis

The kinetic model for the Maillard reaction was developed based on data collected from glucose, glycine, acetic acid, formic acid, and melanoidin measurements. The model was fitted to the experimental data using Copasi® software, which minimized the residuals between the experimental and simulated data using an evolutionary programing algorithm. The model accuracy was evaluated using the R^2 value, which represents the explained variance.

2.9. Statistics

All statistical analyses (DPPH kinetic assay and MR kinetic studies) were performed using Copasi® software. Results are presented as means ± standard deviation, and statistical significance was considered at $p < 0.05$.

3. Results and discussion

3.1. Antioxidant kinetic rate and capacity

This study investigated the formation and reactivity of antioxidants in Maillard Reaction Products (MRPs) using a stopped-flow technique, providing insights into their free radical-scavenging kinetics. Fig. 1a illustrates the stopped-flow apparatus, and Fig. 1b shows the rapid consumption of DPPH• radicals (100 μmol/L) by MRPs (30 μmol/L GAE) after a 4-h reaction at 90 °C in phosphate buffer (pH 6.8). For comparison, the inset shows the DPPH• radicals consumption at equimolar concentrations of ascorbic acid and Trolox, two well-known water-soluble antioxidants.

3.1.1. Antioxidant kinetic rate

MRPs have high free radical-scavenging kinetics, as demonstrated by the rapid decrease in DPPH• radical concentration reported in Fig. 1b. The inset shows a comparison of fast DPPH• reduction by MRPs, Trolox, and ascorbic acid within 5 s. The rate constant k_{DPPH} quantifies the reactivity of antioxidants, providing insights into the effectiveness of MRPs in inhibiting oxidative processes. Recent studies have highlighted the utility of k_{DPPH} values for not only comparing antioxidant reactivity (Shojaee et al., 2022), but also screening for their efficacy in specific food matrices (Angeli et al., 2021), such as the anti-browning mechanism of different apple cultivars (Angeli et al., 2024).

The experiments were designed with antioxidants as the limiting reagents to ensure that only a portion of excess DPPH• was consumed. This setup accurately captures the reaction kinetics using the mechanism given in eqs. (1)–(3). The main reaction (eq. (1)) involves electron transfer between the antioxidant (AH) and the DPPH• radicals to produce the oxidized antioxidant (A•). Although theoretically reversible, the reverse reaction is typically slow for highly effective antioxidants, as noted by Foti et al. (Foti & Daquino, 2006). In addition, side reactions between A• and residual DPPH• (k_{side}) and termination processes via A• dimerization or disproportionation (k_{term}) significantly contribute to the overall mechanism, in particular when dealing with complex extracts, where the main reaction cannot describe completely the kinetics. In fact, in the reaction of DPPH• with the extracts, since these are multicomponent solutions, there are interactions and equilibria that cannot be adequately described with a simple model than include just the main reaction (k_{DPPH}). These complexities emphasize the need for quantitative kinetic studies rather than reliance solely on antioxidant capacity assays (Angeli et al., 2021; Foti et al., 2004).

The rate constant (k_{DPPH}) for the reaction between MRPs and DPPH• radicals was determined to be 6000 ± 300 M^{-1}s^{-1} in methanol/water (80:20). Although this value is approximately half that of ascorbic acid (k_{DPPH} = 14,450 ± 750 mol^{-1} L s^{-1}), it still indicates substantial antioxidant activity. Both MRPs and ascorbic acid had significantly higher k_{DPPH} values than Trolox (k_{DPPH} = 1770 ± 90 mol^{-1} L s^{-1}, $p < 0.05$), indicating greater reactivity. Furthermore, MRPs exhibited higher k_{DPPH} values than other antioxidants, such as rutin, ellagic acid, and quercetin, as reported in previous studies (Angeli et al., 2021; Foti et al., 2004).

The k_{DPPH} for Trolox observed in this study is consistent with the literature values, ranging from 320 mol^{-1} L s^{-1} in pure methanol (Santosh Kumar et al., 2002) to approximately 10^4 mol^{-1} L s^{-1} in ethanol/water mixtures, with variations depending on the water content, which facilitates electron transfer (Friaa & Brault, 2006). The k_{DPPH} value of Trolox measured in this study in methanol/water (80:20) was within this range, indicating the reliability of the experimental approach.

3.1.2. Antioxidant capacity

MRPs exhibited similar antioxidant capacity to ascorbic acid when evaluated via the stoichiometry of their DPPH• reaction. The stoichiometry coefficient n was calculated as $n = \Delta(Abs)/(\Delta\varepsilon \times L \times [AH])$, where $\Delta(Abs)$ is the absorbance change recorded at the end of the

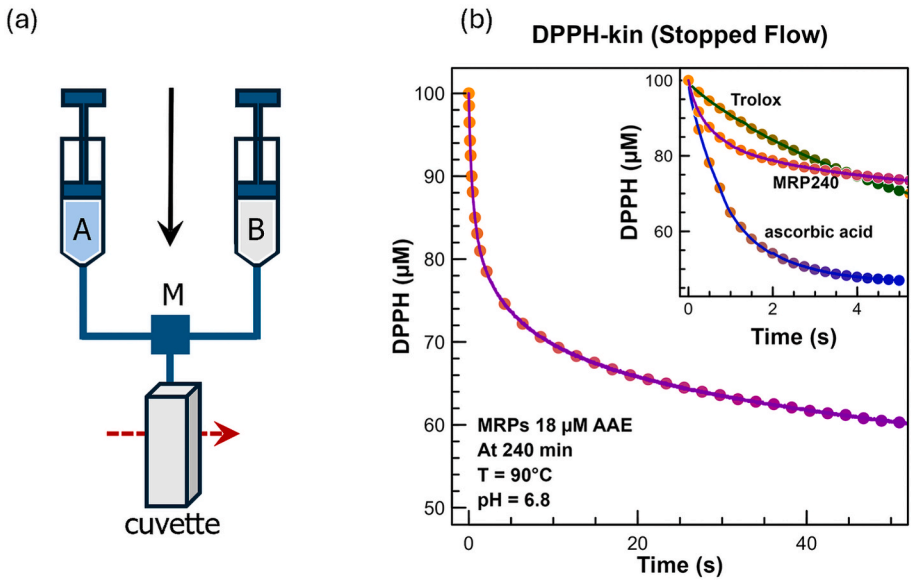

Fig. 1. Results of the kinetic DPPH assay using a stopped-flow technique. (a) Stopped-flow apparatus, including a driving motor, syringes A (filled with DPPH•) and B (filled with the antioxidant), mixer (M), and UV cell. (b) Experimental and simulated kinetic traces of DPPH• reduction by Maillard reaction products. Inset: Zoom of the DPPH• decay within 5 s for MRPs, ascorbic acid, and Trolox. AAE: ascorbic acid equivalent.

reaction, $\Delta\varepsilon$ is the molar extinction coefficient of DPPH•, L is the optical path length, and [AH] is the effective antioxidant concentration. At longer reaction times, when the absorbance signal of DPPH• reaches a steady state, ~ 18 µmol/L ascorbic acid equivalent of MRPs neutralize approximately 30–40 µmol/L of DPPH• radicals, yielding $n \approx 1.8$–2.0. Similarly, 30 µmol/L of ascorbic acid or Trolox neutralize 55–60 µmol/L of DPPH• radicals, giving $n \approx 2.0$, indicating a similar antioxidant capacity of MRPs (at pH 6.8).

The mechanism behind ascorbic acid's stoichiometry involves transferring one electron to DPPH•, forming semi-dehydroascorbic acid, which further reacts with DPPH• to form dehydroascorbic acid (Kamrul et al., 2016). Similarly, Trolox, a vitamin E analog, reacts with DPPH•, forming a Trolox radical that subsequently reacts with another DPPH• radical to complete the neutralization process. The stoichiometry coefficients of Trolox and ascorbic acid are consistent with prior research (Asma et al., 2024).

The apparent stoichiometry value of the MRPs indicates that 1 mol of MRP neutralizes approximately 2 mol of free radicals indicationg that MRPs effectively scavenge free radicals based on k_{DPPH}, and they exhibit a similar antioxidant capacity to ascorbic acid or Trolox. Nevertheless, the high reactivity of MRPs confirm that they play a valuable role in broader antioxidant strategies. These results give an idea of the antioxidant behaviour of MRPs, even if it does not allow the complete characterization of the compounds present in the samples, since they were not separated or isolated. Future studies should explore the antioxidant kinetics of single compounds produced thorough MR and

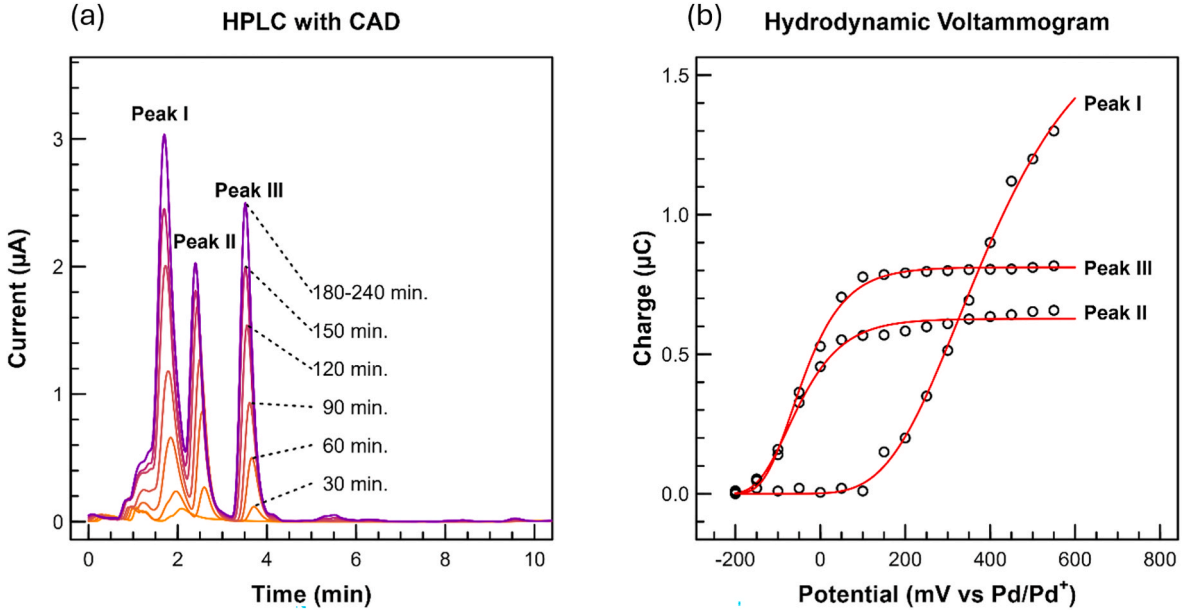

Fig. 2. **(a)** Total current (µA) chromatograms of MRP recorded over 0–240 min of constant heating at 90 °C. Peaks I, II, and III correspond to distinct MR products. **(b)** Hydrodynamic voltammograms (HDVs) of Peaks I, II, and III. The HDVs depict the charge (µC) as a function of the applied potential (mV vs. Pd/Pd + pseudo-reference electrode) for the three peaks identified in the HPLC-CAD chromatograms of the MR samples.

potential synergistic action of these compounds with other antioxidants to enhance overall food stability.

3.2. Electrochemical screening of maillard reaction products

The reactivity of MRPs in scavenging free radicals, as determined by the DPPH assay in hydroalcoholic solvents (pH 6.8), is attributed to their electron-transfer capacity (Gulcin & Alwasel, 2023). This was further investigated using high-performance liquid chromatography (HPLC) coupled with a coulometric array detector (CAD). Fig. 2a shows three main anodic peaks were detected at retention times of 1.5 min (Peak I), 2.25 min (Peak II), and 3.4 min (Peak III). The short retention times of these peaks, observed on a C18 column, suggest that the electroactive species formed in the MRPs are primarily hydrophilic, consistent with the findings of Zielińska on antioxidants in bread crusts (Zielińska et al., 2022).

Only Peaks II and III exhibited significant antioxidant activity as shown in the hydrodynamic voltammograms in Fig. 2b, recorded at pH 3.0. Peaks II and III displayed the lowest half-wave potentials ($E_{1/2}$), indicating strong electron-donating abilities. Peaks II and III had $E_{1/2}$ values of −50 mV vs. Pd reference electrode (equivalent to +507 mV vs. the standard hydrogen electrode (SHE)) was significantly lower than Peak I ($E_{1/2}$ of +957 mV vs. SHE, $p < 0.05$), demonstrating superior antioxidant potential.

In electrochemical analyses, lower $E_{1/2}$ values correlate with enhanced electron donation, a key trait of efficient antioxidants (Chevion et al., 2000). The low $E_{1/2}$ values of Peaks II and III, compared with those of ascorbic acid ($E_{1/2}$ = +657 mV vs. SHE at pH 3.0) (Ding et al., 2022; Gazdik et al., 2008; Razem et al., 2022) suggest that these species are potent antioxidants.

3.3. Tentative identification of antioxidants in maillard reaction products

The mass spectra of Peaks II and III show the same molecular ion with a mass-to-charge ratio (m/z) of 145.0496, suggesting two similar molecules with different retention times. The fragmentation pattern exhibited a major peak at m/z 71.0492, indicating of a stable fragment. Other fragments (m/z 127.0390, 99.0441, and 71.0492) align with water and carbon monoxide losses. Studies on 1-deoxyglucosone (1-DG) degradation under neutral or alkaline conditions have reported the formation of 3,5-dihydroxy-6-methyl-2,3-dihydro-4H-pyran-4-one (DDMP) and its furanone isomer (Chen et al., 2021; Li et al., 2019). The chemical structure reported in Fig. 3 is consistent with the observed fragmentation patterns of Peaks II and III. DDMP is also the major product of the reaction of glucose and proline (Mori & Ito, 2004) and is found in several foods (Qiao et al., 2022).

UV spectral analysis (Supporting information S1) revealed absorption maxat 290 nm for both Peaks II and III, consistent with an enone group and suggesting a structure containing ketone and double bonds. The pyranone and furanone isomers likely contributed to the antioxidant properties observed in the DPPH-kin assays, consistent with their low half-wave potential. This finding aligns with studies showing that reductone structures, like DDMP, facilitate electron donation and neutralize free radicals (Chen et al., 2021; Kanzler et al., 2016; X. Yu et al., 2013).

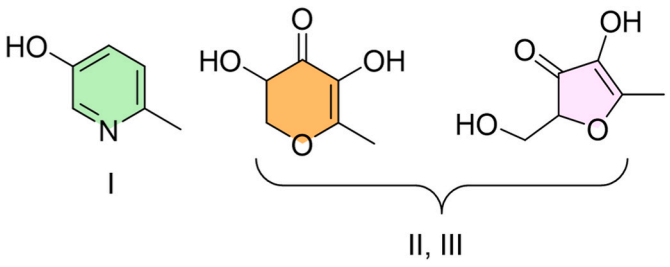

Fig. 3. Structures assigned through HRMS to the three peaks exhibiting antioxidant activity. Peak I, in green, corresponds to 6-methylpyridin-3-ol (MP), while peak II (orange) and peak III (violet) correspond to 3,5-dihydroxy-6-methyl-2,3-dihydro-4H-pyran-4-one (DDMP) and its furanone isomer.

Peak I exhibited a molecular ion at m/z 110.0601. Fragments (m/z 94.0530, 82.0650, and 66.0420) suggested methyl groups and carbon monoxide loss. The molecular formula of the compound was identified as C_6H_7NO, and its structure, shown in Fig. 3, was proposed as 6-methylpyridin-3-ol (MP), based on mass spectral databases (m/z Cloud and ChemSpider). Peak I exhibited modest antioxidant activity, consistent with the well-known weak reactivity of pyridine derivatives with radicals (Kanzler et al., 2016, 2017; Yanagimoto et al., 2002).

3.4. Kinetic modeling of antioxidant evolution during the maillard reaction

To explain the formation of antioxidants during the Maillard reaction, a kinetic model was developed based on monitoring key intermediates using NMR spectroscopy. Fig. 4 presents the NMR traces showing the consumption of 200 mmol/L glucose and glycine, along with the formation of acetate, formate, and melanoidins over time. Notably, the pH dropped from 6.8 to 5.2, indicating increased acid formation, consistent with previous findings (Mori & Ito, 2004).

This model simplifies and builds upon previously reported mechanisms (Lund & Ray, 2017; Martins & Van Boekel, 2005). As shown in Table 1, the model captures key pathways of the Maillard reaction, including glucose isomerization to fructose, higher glucose consumption relative to glycine, and greater formation of acetic acid compared to formic acid and melanoidins. The observed increase in fructose concentration (2–5 mmol/L) is attributed to glucose isomerization (Delidovich, 2023), whereas the higher glucose consumption relative to glycine, as demonstrated in Fig. 5a, results from the regeneration of glycine from Amadori products (Martins & Van Boekel, 2005).

Melanoidins formation at 4 mmol/L as reported in Fig. 5b, was confirmed through visible spectroscopy (extinction coefficient = 0.64 mol^{-1} L cm^{-1}) (Martins & Van Boekel, 2003). Acetic acid concentrations consistently exceeded those of formic acid, indicating the predominance of the 2,3-enolization pathway. The minimal formation of formic acid and the absence of significant 3-deoxyglucosone (3-DG) degradation product 5-hydroxymethylfurfural (HMF) (Lee et al., 2022), suggest that the 1,2-enolization pathway is negligible under these conditions (Yaylayan & Keyhani, 2000). The neutral pH, which disfavors 3-DG formation, further supports this conclusion.

The iterative fitting procedure described in the experimental section was employed to refine the kinetic model using nonlinear regression. The strong correlation between simulated and experimental values ($R^2 > 0.99$) confirms that the model can describe the Maillard reaction.

The key steps in the kinetic model are summarized as follow.

1. **Glucose Degradation:** Glucose degrades into formic acid (FA) and acetic acid (AA) with a rate constant $k_1 = 0.733\ s^{-1}$, comparable to values reported by Martins and Van Boekel (2005) ($p > 0.05$).
2. **Glucose Isomerization:** Glucose isomerizes to fructose in a reversible reaction with the forward and backward rate constants k_{2f} and k_{2b}, respectively. The high backward rate constant (88 s^{-1}) indicates limited isomerization after 4 h of heating.
3. **Amadori Product Formation:** Glucose and glycine react to form Amadori rearrangement products (ARP) with a fixed rate constant $k_3 = 0.097\ mol^{-1}$ L s^{-1}. These ARPs eventually degrade to produce antioxidant species.
4. **1-DG Formation:** ARP breaks down to 1-deoxyglucosone (1-DG) while regenerating glycine. This step is crucial because 1-DG serves as a precursor for antioxidant species and melanoidins.
5. **Further Degradation of 1-DG:** 1-DG was further degraded to acetic acid and erythrose with a rate constant $k_5 = 383\ s^{-1}$.

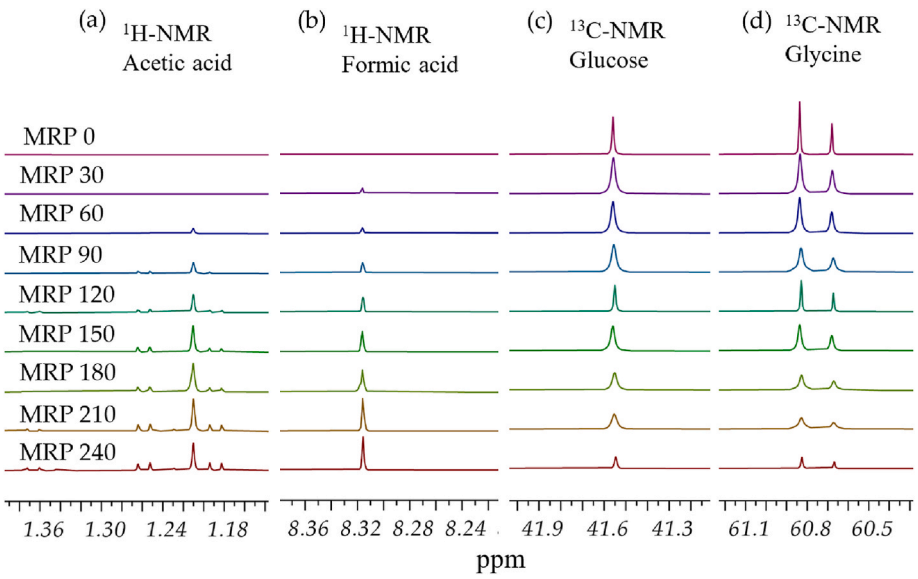

Fig. 4. (a) Stacked ^{1}H-NMR peak corresponding to acetic acid obtained from MR samples incubated for 0, 120, and 240 min at 90 °C; (b) Stacked ^{1}H-NMR peak corresponding to formic acid obtained from MR samples incubated for 0, 120, and 240 min at 90 °C; (c) Stacked ^{13}C-NMR peak corresponding to glucose obtained from MR samples incubated for 0, 120, and 240 min at 90 °C; (d) Stacked ^{13}C-NMR peak corresponding to glycine obtained from MR samples incubated for 0, 120, and 240 min at 90 °C.

Table 1
Rate constants relative to the kinetic model of MR reported by Martins & Van Boekel, 2005, and obtained fitting the same model to the data measured in this work and the %RDS. Abbreviations: formic acid (FA); acetic acid (AA); Amadori products (ARP); 1-deoxyglucosone (1-DG); browning products, such as melanoidins (B).

Rxn.	Elementary step	Symbol	Units	(Martins & Van Boekel, 2005) x10^{6}	This work x10^{6}	RSD (%)
(1)	glucose → FA + AA	k_1	s^{-1}	0.716	0.733	2
(2)	glucose ⇆ fructose	k_{2f}	s^{-1}	6.83	0.016	ind.
		k_{2b}	s^{-1}	58.3	88	29
(3)	glucose + glycine → ARP	k_3	mol^{-1} L s^{-1}	0.097	0.097	–
(4)	ARP → 1-DG + glycine	k_4	s^{-1}	111	225	4
(5)	1-DG → AA + erythrose	k_5	s^{-1}	383	383	–
(6)	1-DG + glycine → brown products	k_6	mol^{-1} L s^{-1}	320	0.038	2
(7)	1-DG → AH	k_7	s^{-1}		1480	6
(8)	AH → brown products	k_8	s^{-1}		113	12

Note: when RSD is missing (−), the rate constant is fixed as in the VB calculation.

6. **Melanoidin Formation:** 1-DG and glycine react to form melanoidins, contributing to the characteristic browning and antioxidant activity of Maillard products. The rate constant in this study was estimated at $k_6 = 0.038$ mol^{-1} L^{-1}, significantly lower than previously reported values (Martins & Van Boekel, 2005), possibly due to the oxidation of antioxidants (see Step 8).

Two additional key steps were included to describe the formation of antioxidants during the Maillard reaction.

7. **Antioxidant Formation:** 1-DG is converted into antioxidant species (AH) in reduced form ("red"), with a rate constant $k_7 = 1480$ s^{-1}. These antioxidants play critical roles in the radical scavenging properties of MRPs, with DDMP and its furanone tautomer being the most significant contributors, as previously described.
8. **Antioxidant Degradation:** The degradation of antioxidant species (AH) occurs with a rate constant $k_8 = 113$ s^{-1}. The balance between formation and degradation results in a production curve in which antioxidant levels plateau as degradation begins to dominate. This process also contributes to non-enzymatic browning.

Fig. 5c illustrates the trend in antioxidant species formation predicted by the model, which aligns with HPLC-CAD analysis results. The model's accuracy was further demonstrated by its strong correlation with experimental data ($R^2 > 0.99$). These findings indicate that optimizing the Maillard reaction during food processing can enhance antioxidant production, leading to the development of food products with improved stability.

4. Conclusions

This study investigated the formation, kinetic behavior, and antioxidant activity of Maillard reaction products (MRPs) generated from the reaction between glucose and glycine under controlled conditions (90 °C and pH 6.8). The results revealed significant consumption of glucose and glycine, leading to the formation of key MRPs, including acetic acid, formic acid, and melanoidins.

A simplified kinetic model was developed and validated using experimental data and numerical simulations.

The antioxidant capacity of MRPs, as assessed using the DPPH assay, exhibited a trend characterized by rapid reaction kinetics and high antioxidant values, underscoring their potential application in food systems where swift neutralization of reactive oxygen species is desirable. This behavior was incorporated into the kinetic model.HPLC-CAD analysis confirmed that the production of DDMP, its furanone tautomer and MPO were contributors to antioxidant activity.

The rapid reactivity of MRPs measured with DPPH assay kinetic approach suggests that MRPs could serve as effective natural antioxidants.These results underscore the importance of specific MRPs,

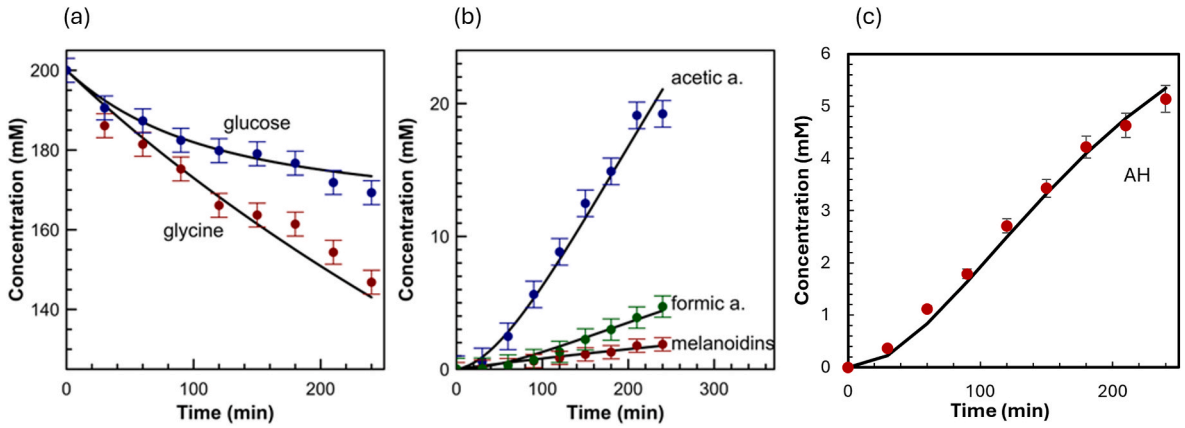

Fig. 5. Fits to experimental data (colored dots) with the updated kinetic model based on Martins & Van Boekel, 2005 (black lines) of (a) reactants (glucose, glycine) and (b) products (formic acid, acetic acid and melanoidins) using Copasi software. (c) Trend of antioxidant species formation during Maillard reaction measured (red dots) and fitted by the kinetic model (black line).

particularly DDMP and its isomer, in significantly boosting the overall antioxidant capacity of the system.

In conclusion, this study enhances our understanding of the formation, reactivity, and antioxidant potential of MRPs. These findings demonstrate that MRPs can inhibit oxidative deterioration, extend the shelf life, and improve overall food quality. While this study focused on specific temperature and pH conditions, it is reasonable to speculate that optimizing these reaction parameters could further enhance the formation of desirable antioxidants while minimizing the production of less favorable byproducts. These insights have important implications for the development of naturally derived food additives, particularly in the context of "clean label" products, where there is growing demand for natural alternatives to synthetic additives. Future research should focus on further elucidating the mechanisms governing MRP formation and degradation, and exploring their potential applications in food science and nutrition under varying processing conditions.

CRediT authorship contribution statement

Sara Bolchini: Writing – original draft, Visualization, Investigation, Formal analysis. **Lucrezia Angeli:** Methodology. **Giovanna Ferrentino:** Writing – review & editing. **M.A.J.S. Van Boekel:** Writing – review & editing. **Riccardo Amorati:** Writing – review & editing. **Matteo Scampicchio:** Writing – review & editing, Supervision, Software, Formal analysis, Conceptualization. **Ksenia Morozova:** Writing – review & editing, Supervision, Methodology, Investigation.

Declaration of competing interest

The authors declare that they have no known competing financial interests or personal relationships that could have appeared to influence the work reported in this paper.

Acknowledgements

Award Number: Project code PE00000003, Concession Decree No. 1550 of October 11, 2022 adopted by the Italian Ministry of University and Research, CUP D93C22000890001, Project title “ON Foods – Research and innovation network on food and nutrition Sustainability, Safety and Security – Working ON Foods”. This work was supported by the Open Access Publishing Fund of the Free University of Bozen-Bolzano.

Appendix A. Supplementary data

Supplementary data to this article can be found online at https://doi.org/10.1016/j.lwt.2024.117316.

Data availability

Data are available upon request from the authors.

References

Amorati, R., & Valgimigli, L. (2018). Methods to measure the antioxidant activity of phytochemicals and plant extracts. *Journal of Agricultural and Food Chemistry, 66* (13), 3324–3329. https://doi.org/10.1021/acs.jafc.8b01079

Angeli, L., Imperiale, S., Ding, Y., Scampicchio, M., & Morozova, K. (2021). A novel stoichio-kinetic model for the dpph• assay: The importance of the side reaction and application to complex mixtures. *Antioxidants, 10*(7), 16–20. https://doi.org/10.3390/antiox10071019

Angeli, L., Populin, F., Morozova, K., Ding, Y., Asma, U., Bolchini, S., Cebulj, A., Busatto, N., Costa, F., Ferrentino, G., & Scampicchio, M. (2024). Comparative analysis of antioxidant activity and capacity in apple varieties: Insights from stopped flow DPPH• kinetics, mass spectrometry and electrochemistry. *Food Bioscience, 58* (December 2023), Article 103729. https://doi.org/10.1016/j.fbio.2024.103729

Asma, U., Bertotti, M. L., Zamai, S., Arnold, M., Amorati, R., & Scampicchio, M. (2024). A kinetic approach to oxygen radical absorbance capacity (ORAC): Restoring order to the antioxidant activity of hydroxycinnamic acids and fruit juices. *Antioxidants, 13* (2), 222. https://doi.org/10.3390/antiox13020222

Cao, J., Yan, H., & Liu, L. (2022). Optimized preparation and antioxidant activity of glucose-lysine Maillard reaction products. *LWT - Food Science and Technology, 161* (September 2021), Article 113343. https://doi.org/10.1016/j.lwt.2022.113343

Chen, Z., Xi, G., Fu, Y., Wang, Q., Cai, L., Zhao, Z., Liu, Q., Bai, B., & Ma, Y. (2021). Synthesis of 2,3-dihydro-3,5-dihydroxy-6-methyl-4H-pyran-4-one from maltol and its taste identification. *Food Chemistry, 361*(March), Article 130052. https://doi.org/10.1016/j.foodchem.2021.130052

Chevion, S., Roberts, M. A., & Chevion, M. (2000). The use of cyclic voltammetry for the evaluation of antioxidant capacity. *Free Radical Biology and Medicine, 28*(6), 860–870. https://doi.org/10.1016/S0891-5849(00)00178-7

Delidovich, I. (2023). Toward understanding base-catalyzed isomerization of saccharides. *ACS Catalysis, 13*(4), 2250–2267. https://doi.org/10.1021/acscatal.2c04786

Ding, Y., Morozova, K., Imperiale, S., Angeli, L., Asma, U., Ferrentino, G., & Scampicchio, M. (2022). HPLC-Triple detector (Coulometric array, diode array and mass spectrometer) for the analysis of antioxidants in officinal plants. *LWT - Food Science and Technology, 162*(April), Article 113456. https://doi.org/10.1016/j.lwt.2022.113456

Everette, J. D., Bryant, Q. M., Green, A. M., Abbey, Y. A., Wangila, G. W., & Walker, R. B. (2010). Thorough study of reactivity of various compound classes toward the folin-Ciocalteu reagent. *Journal of Agricultural and Food Chemistry, 58*(14), 8139–8144. https://doi.org/10.1021/jf1005935

Feng, J., Berton-Carabin, C. C., Fogliano, V., & Schroën, K. (2022). Maillard reaction products as functional components in oil-in-water emulsions: A review highlighting interfacial and antioxidant properties. *Trends in Food Science and Technology, 121* (February), 129–141. https://doi.org/10.1016/j.tifs.2022.02.008

Foti, M. C. (2015). Use and abuse of the DPPH• radical. *Journal of Agricultural and Food Chemistry, 63*(40), 8765–8776. https://doi.org/10.1021/ACS.JAFC.5B03839

Foti, M. C., & Daquino, C. (2006). Kinetic and thermodynamic parameters for the equilibrium reactions of phenols with the dpph. radical. *Chemical Communications, 30*, 3252–3254. https://doi.org/10.1039/b606322e

Foti, M. C., Daquino, C., & Geraci, C. (2004). Electron-transfer reaction of cinnamic acids and their methyl esters with the DPPH. Radical in alcoholic solutions. *Journal of*

Organic Chemistry, 69(7), 2309–2314. https://doi.org/10.1021/JO035758Q/SUPPL_FILE/JO035758QSI20040113_051425.PDF

Friaa, O., & Brault, D. (2006). Kinetics of the reaction between the antioxidant Trolox® and the free radical DPPH• in semi-aqueous solution. *Organic and Biomolecular Chemistry, 4*(12), 2417–2423. https://doi.org/10.1039/b602147f

Gazdik, Z., Zitka, O., Petrlova, J., Adam, V., Zehnalek, J., Horna, A., Reznicek, V., Beklova, M., & Kizek, R. (2008). Determination of vitamin C (ascorbic acid) using high performance liquid chromatography coupled with electrochemical detection. *Sensors, 8*(11), 7097–7112. https://doi.org/10.3390/s8117097

Gulcin, İ., & Alwasel, S. H. (2023). DPPH radical scavenging assay. *Processes, 11*(8). https://doi.org/10.3390/pr11082248

Habinshuti, I., Chen, X., Yu, J., Mukeshimana, O., Duhoranimana, E., Karangwa, E., Muhoza, B., Zhang, M., Xia, S., & Zhang, X. (2019). Antimicrobial, antioxidant and sensory properties of Maillard reaction products (MRPs) derived from sunflower, soybean and corn meal hydrolysates. *LWT - Food Science and Technology, 101*(July 2018), 694–702. https://doi.org/10.1016/j.lwt.2018.11.083

Han, Z., Zhu, M., Wan, X., Zhai, X., Ho, C., & Zhang, L. (2022). Food polyphenols and maillard reaction: Regulation effect and chemical mechanism. *Critical Reviews in Food Science and Nutrition*.

Jia, W., Guo, A., Zhang, R., & Shi, L. (2023). Mechanism of natural antioxidants regulating advanced glycosylation end products of Maillard reaction. *Food Chemistry, 404*(PA), Article 134541. https://doi.org/10.1016/j.foodchem.2022.134541

Kamrul, H. S. M., Schiraldi, A., Cosio, M. S., & Scampicchio, M. (2016). Food and ascorbic scavengers of hydrogen peroxide: A reaction calorimetry investigation. *Journal of Thermal Analysis and Calorimetry, 125*(2), 729–737. https://doi.org/10.1007/s10973-015-5170-3

Kanzler, C., Haase, P. T., Schestkowa, H., & Kroh, L. W. (2016). Antioxidant properties of heterocyclic intermediates of the maillard reaction and structurally related compounds. *Journal of Agricultural and Food Chemistry, 64*(41), 7829–7837. https://doi.org/10.1021/acs.jafc.6b03398

Kanzler, C., Schestkowa, H., Haase, P. T., & Kroh, L. W. (2017). Formation of reactive intermediates, color, and antioxidant activity in the maillard reaction of maltose in comparison to d -glucose. *Journal of Agricultural and Food Chemistry, 65*(40), 8957–8965. https://doi.org/10.1021/acs.jafc.7b04105

Kitts, D. D. (2021). Antioxidant and functional activities of mrps derived from different sugar–amino acid combinations and reaction conditions. *Antioxidants, 10*(11). https://doi.org/10.3390/antiox10111840

Lee, J., Roux, S., Le Roux, E., Keller, S., Rega, B., & Bonazzi, C. (2022). Unravelling caramelization and Maillard reactions in glucose and glucose + leucine model cakes: Formation and degradation kinetics of precursors, α-dicarbonyl intermediates and furanic compounds during baking. *Food Chemistry, 376*(December 2021), Article 131917. https://doi.org/10.1016/j.foodchem.2021.131917

Li, H., Tang, X. Y., Wu, C. J., & Yu, S. J. (2019). Formation of 2,3-dihydro-3,5-Dihydroxy-6-Methyl-4(H)-Pyran-4-One (DDMP) in glucose-amino acids Maillard reaction by dry-heating in comparison to wet-heating. *LWT - Food Science and Technology, 105*(October 2018), 156–163. https://doi.org/10.1016/j.lwt.2019.02.015

Lund, M. N., & Ray, C. A. (2017). Control of maillard reactions in foods: Strategies and chemical mechanisms. *Journal of Agricultural and Food Chemistry, 65*(23), 4537–4552. https://doi.org/10.1021/acs.jafc.7b00882

Martins, S. I. F. S., & Van Boekel, M. A. J. S. (2003). Melanoidins extinction coefficient in the glucose/glycine Maillard reaction. *Food Chemistry, 83*(1), 135–142. https://doi.org/10.1016/S0308-8146(03)00219-X

Martins, S. I. F. S., & Van Boekel, M. A. J. S. (2005). A kinetic model for the glucose/glycine Maillard reaction pathways. *Food Chemistry, 90*(1–2), 257–269. https://doi.org/10.1016/j.foodchem.2004.04.006

Mildner-Szkudlarz, S., Barbara Różańska, M., Siger, A., Zembrzuska, J., & Szwengiel, A. (2023). Formation of Maillard reaction products in a model bread system of different gluten-free flours. *Food Chemistry, 429*(January). https://doi.org/10.1016/j.foodchem.2023.136994

Monti, S. M., Ritieni, A., Graziani, G., Randazzo, G., Mannina, L., Segre, A. L., & Fogliano, V. (1999). LC/MS analysis and antioxidative efficiency of Maillard reaction products from a lactose-lysine model system. *Journal of Agricultural and Food Chemistry, 47*(4), 1506–1513. https://doi.org/10.1021/jf980899s

Mori, M., & Ito, K. (2004). Effects of pH on the formation of volatile products in non-enzymatic browning of maltose. *Food Science and Technology Research, 10*(1), 60–64. https://doi.org/10.3136/fstr.10.60

Nooshkam, M., Varidi, M., & Bashash, M. (2019). The Maillard reaction products as food-born antioxidant and antibrowning agents in model and real food systems. *Food Chemistry, 275*(September 2018), 644–660. https://doi.org/10.1016/j.foodchem.2018.09.083

Qiao, Y., Bi, J., Chen, Q., Wu, X., Jin, X., Gou, M., Yang, X., & Purcaro, G. (2022). Rapid and sensitive quantitation of DDMP (2,3-dihydro-3,5-dihydroxy-6-methyl-4H-pyran-4-one) in baked red jujubes by HS-SPME-GC-MS/MS. *Food Control, 135*(July 2021), Article 108820. https://doi.org/10.1016/j.foodcont.2022.108820

Razem, M., Ding, Y., Morozova, K., Mazzetto, F., & Scampicchio, M. (2022). Analysis of phenolic compounds in food by coulometric array detector: A review. *Sensors, 22*(19). https://doi.org/10.3390/s22197498

Santosh Kumar, S., Priyadarsini, K. I., & Sainis, K. B. (2002). Free radical scavenging activity of vanillin and o-vanillin using 1,1-diphenyl-2-picrylhydrazyl (DPPH) radical. *Redox Report, 7*(1), 35–40. https://doi.org/10.1179/135100002125000163

Shakoor, A., Zhang, C., Xie, J., & Yang, X. (2022). Maillard reaction chemistry in formation of critical intermediates and flavour compounds and their antioxidant properties. *Food Chemistry, 393*(May), Article 133416. https://doi.org/10.1016/j.foodchem.2022.133416

Shojaee, M. S., Moeenfard, M., & Farhoosh, R. (2022). Kinetics and stoichiometry of gallic acid and methyl gallate in scavenging DPPH radical as affected by the reaction solvent. *Scientific Reports, 12*(1), 1–9. https://doi.org/10.1038/s41598-022-12803-3

Sohail, A., Al-Dalali, S., Wang, J., Xie, J., Shakoor, A., Asimi, S., Shah, H., & Patil, P. (2022). Aroma compounds identified in cooked meat: A review. *Food Research International, 157*(April), Article 111385. https://doi.org/10.1016/j.foodres.2022.111385

Sun, A., Chen, L., Wu, W., Soladoye, O. P., Zhang, Y., & Fu, Y. (2023). The potential meat flavoring generated from Maillard reaction products of wheat gluten protein hydrolysates-xylose: Impacts of different thermal treatment temperatures on flavor. *Food Research International, 165*(January). https://doi.org/10.1016/j.foodres.2023.112512

Sun, A., Wu, W., Soladoye, O. P., Aluko, R. E., Bak, K. H., Fu, Y., & Zhang, Y. (2022). Maillard reaction of food-derived peptides as a potential route to generate meat flavor compounds: A review. *Food Research International, 151*(October 2021). https://doi.org/10.1016/j.foodres.2021.110823

Tang, Y., Huang, Y., Li, M., Zhu, W., Zhang, W., Luo, S., Zhang, Y., Ma, J., & Jiang, Y. (2024). Balancing Maillard reaction products formation and antioxidant activities for improved sensory quality and health benefit properties of pan baked buns. *Food Research International, 195*(April), Article 114984. https://doi.org/10.1016/j.foodres.2024.114984

Yanagimoto, K., Lee, K. G., Ochi, H., & Shibamoto, T. (2002). Antioxidative activity of heterocyclic compounds formed in Maillard reaction products. *International Congress Series, 1245*(C), 335–340. https://doi.org/10.1016/S0531-5131(02)01007-5

Yaylayan, V. A., & Keyhani, A. (2000). Origin of carbohydrate degradation products in L-alanine/D- [13C]glucose model systems. *Journal of Agricultural and Food Chemistry, 48*(6), 2415–2419. https://doi.org/10.1021/jf000004n

Yu, M., He, S., Tang, M., Zhang, Z., Zhu, Y., & Sun, H. (2018). Antioxidant activity and sensory characteristics of Maillard reaction products derived from different peptide fractions of soybean meal hydrolysate. *Food Chemistry, 243*(September 2017), 249–257. https://doi.org/10.1016/j.foodchem.2017.09.139

Yu, X., Zhao, M., Liu, F., Zeng, S., & Hu, J. (2013). Identification of 2,3-dihydro-3,5-dihydroxy-6-methyl-4H-pyran-4-one as a strong antioxidant in glucose-histidine Maillard reaction products. *Food Research International, 51*(1), 397–403. https://doi.org/10.1016/j.foodres.2012.12.044

Zielińska, D., Zieliński, H., & Piskuła, M. K. (2022). An electrochemical determination of the total reducing capacity of wheat, spelt, and rye breads. *Antioxidants, 11*(8). https://doi.org/10.3390/antiox11081438